Supporting Information

Plasmonic Properties of Multispot Copper-Capped Nanoparticle Array Chip and Its Application to Optical Biosensor for Pathogen Detection of Multiplex DNAs

Do-Kyun Kim,[†,□] Seung Min Yoo,[†,ϕ,□] Tae Jung Park,[*,†,¶] Hiroyuki Yoshikawa,[‡] Eiichi Tamiya,[‡] Jung Youn Park,[§] and Sang Yup Lee[*,†,ϕ]

[†]BioProcess Engineering Research Center, Center for Systems & Synthetic Biotechnology, and Institute for the BioCentury, KAIST, 291 Daehak-ro, Yuseong-gu, Daejeon 305-701, Republic of Korea, [¶]Center for Nanobio Integration & Convergence Engineering, National Nanofab Center, 291 Daehak-ro, Yuseong-gu, Daejeon 305-806, Republic of Korea, [‡]Department of Applied Physics, Graduate School of Engineering, Osaka University, 2-1 Yamadaoka, Suita, Osaka 565-0871, Japan, [§]Biotechnology Research Division, National Fisheries Research & Development Institute (NFRDI), 408-1 Sirang-ri, Gijang, Busan 619-705, Republic of Korea, [ϕ]Department of Chemical & Biomolecular Engineering (BK21), Department of Bio & Brain Engineering, Department of Biological Sciences, and Bioinformatics Research Center, KAIST, 291 Daehak-ro, Yuseong-gu, Daejeon 305-701, Republic of Korea

Table S1. Average Number of Nanoparticles per Unit Area, Average Number of Nanoparticles per One Spot, and Surface Coverage of Nanoaprticles on the MC-NPA Chip Surface*

nanoparticles per mm^2	**nanoparticls per spot**	**surface coverage of nanoparticles**
7.2×10^7 particles/mm^2	1.4×10^9 particles/spot	56.6% ± 3.5%

*The average number nanoparticles per unit area and the surface coverage of nanoparticles were calculated from the SEM image shown in **Figure S1**. The average number of nanoparticles per spot (radius of 2.5 mm) was calculated accordingly.

Table S2. Bacterial Species Used in This Study

species	**source**
Vibrio vulnificus	KCTC[a] 2962
Salmonella spp.	Clinical isolate
Staphylococcus aureus	KCTC 1621
Staphylococcus epidermidis	KCTC 1917
Enterococcus faecalis	KCCM[b]12117
Klebsiella oxytoca	ATCC[c] 43863
Neisseria gonorrhoea	ATCC 10150

[a]KCTC, Korean Collection for Type Cultures, Daejeon, Korea

[b]KCCM, Korean Culture Center of Microorganisms, Seoul, Korea

[c]ATCC, American Type Culture Collection, Manassas, VA, USA

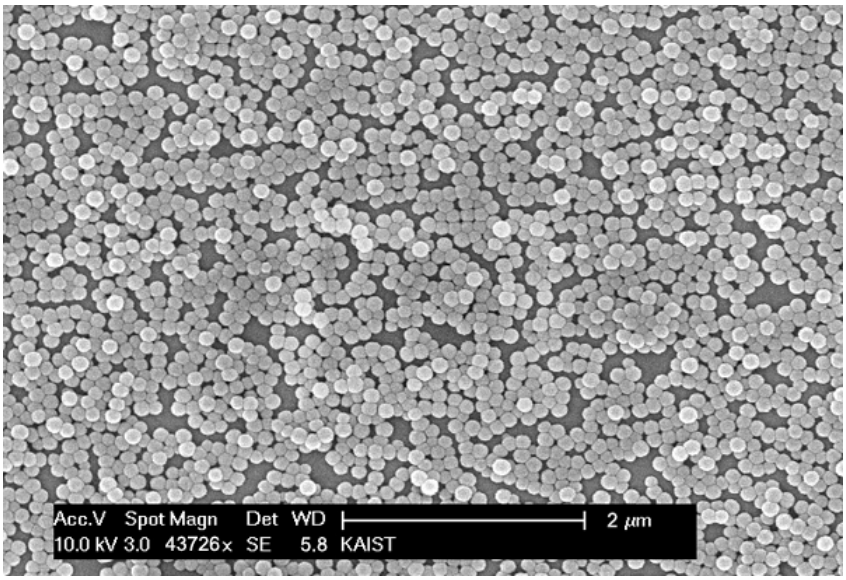

Figure S1. SEM image of MC-NPA chip surface.

Optical Measurement System. The optical measurement system for the evaluation of the optical properties on the MC-NPA chip was based on a spectroscopy system (Ocean Optics). The optical measurement system was consisted with a light source (wavelength range of 360–2000 nm), spectrophotometer (wavelength range of 200–1100 nm) and an optical fiber probe bundle (fiber core diameter: 300 μm, wavelength range of 250–900 nm). Basically, white light, emerging from an optical fiber bundle provided incident light, and this light was reflected upon hitting the chip surface coupled into the detection probe of the optical fiber bundle and analyzed by a spectrometer. The optical property evaluation of the MC-NPA chip was carried out in the wavelength range 400 to 750 nm using the optical measurement system at RT.

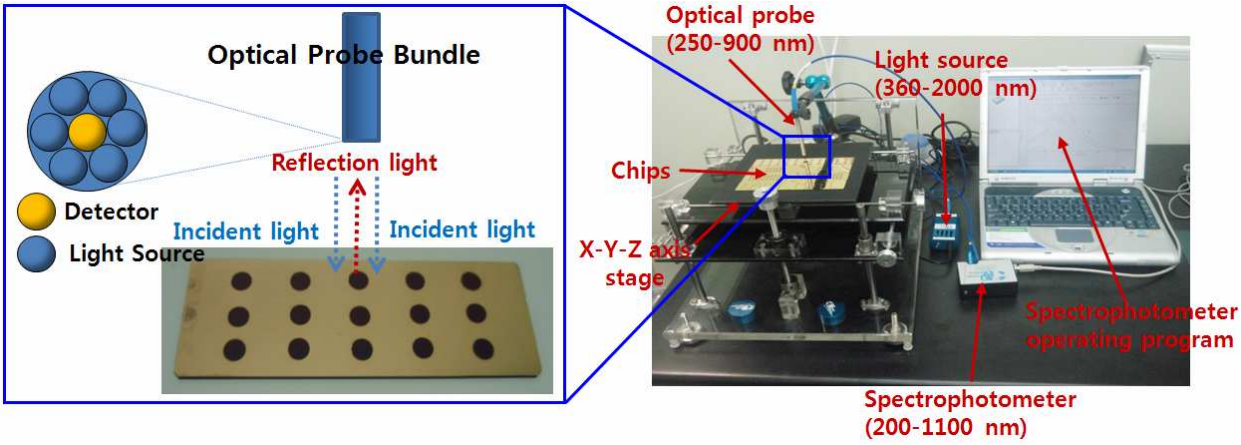

Figure S2. Experimental setup and the optical measurement system for the LSPR-based MC-NPA chip. The optical measurement system for the evaluation of the optical properties on the MC-NPA chip was based on a spectroscopy system.

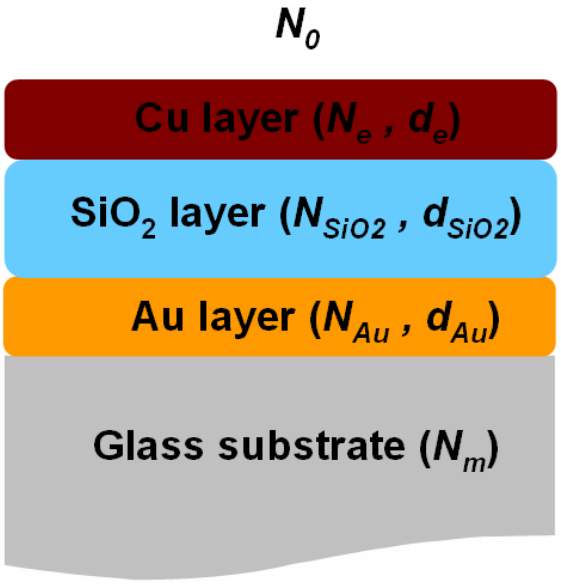

Figure S3. Schematic diagram illustrating the multilayer model for the description of simulation data from Cu-layer/SiO_2-layer/Au-layer/glass substrate composite structures. Here, *N* is a refractive index (RI) and *d* is a thickness of each layer. The RI of a porous Cu film is calculated by using Maxwell-Garnett effective medium theory. Reflection and extinction spectra can be also calculated by using the characteristic matrix of each layer.

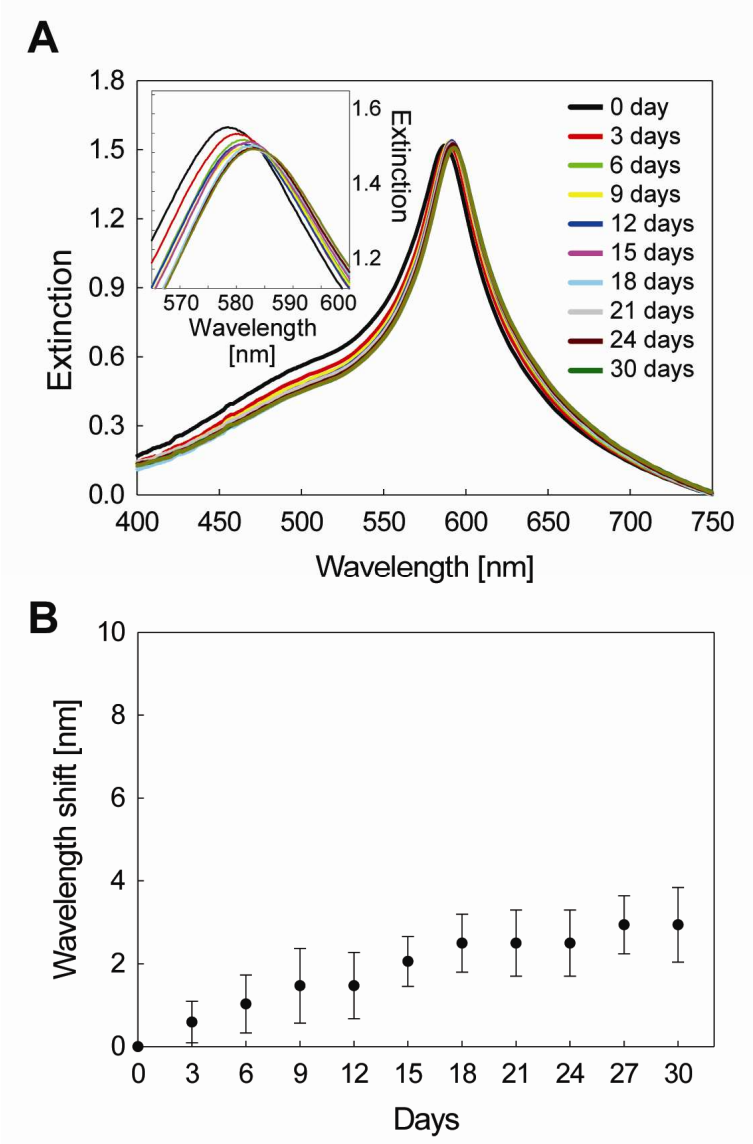

Figure S4. Stability test of MC-NPA chips under ambient condition. MC-NPA chip was incubated at RT with 30% humidity for 30 days and the LSPR spectrum were measured once every three days. (A) Spectrum profiles of MC-NPA chip is shown in the left illustrations and are magnified (inset). (B) Plot of wavelength shift versus incubation day.

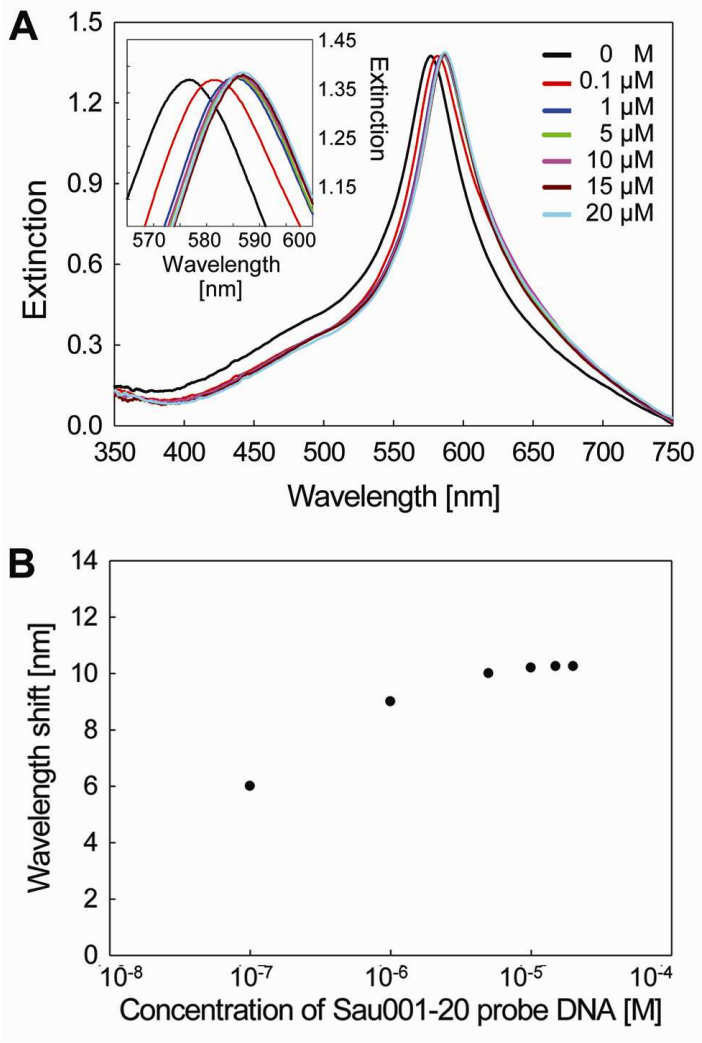

Figure S5. Effect for the concentration of probe DNAs on the LSPR wavelength shift. The spots of MC-NPA chip were assembled with the different concentration of probe DNAs (20, 15, 10, 5, 1 and 0.1 μM, respectively) and then hybridized with target DNAs. (A) LSPR Spectrum profiles of chips and the magnified spectrum profiles (inset). (B) Plot of LSPR wavelength shift versus the concentration of probe DNA.

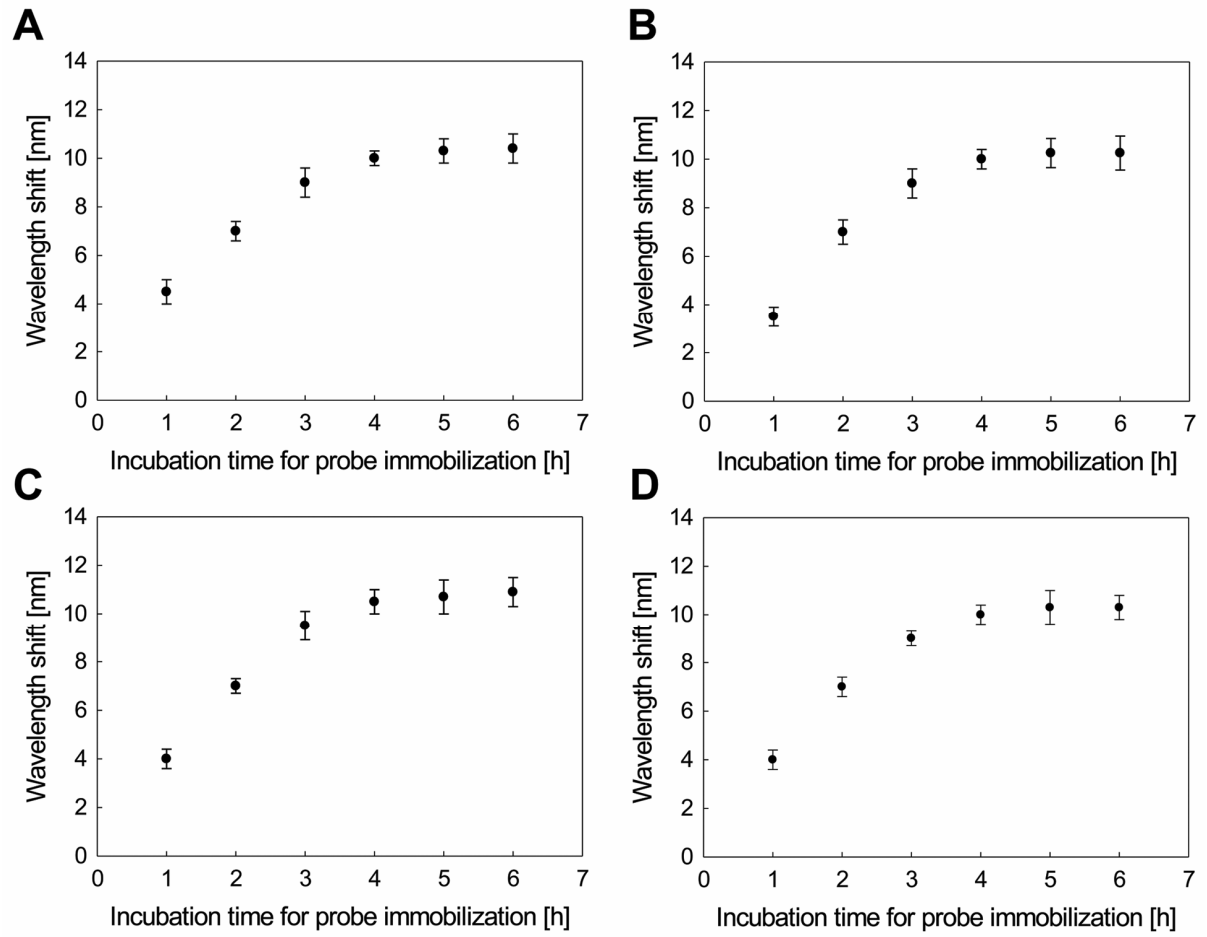

Figure S6. Effect of the incubation time for the immobilization of probe DNAs on the LSPR wavelength shift. The 10 μM probe DNAs were treated on the MC-NPA chip for the different incubation time (1, 2, 3, 4, 5 and 6 h, respectively), and then hybridized with target DNAs, (A) Efm003-20, (B) Sau001-20, (C) Smal03-20 and (D) Vvul02-20, respectively. The data were obtained from three measurements and the error bars represent standard deviation.

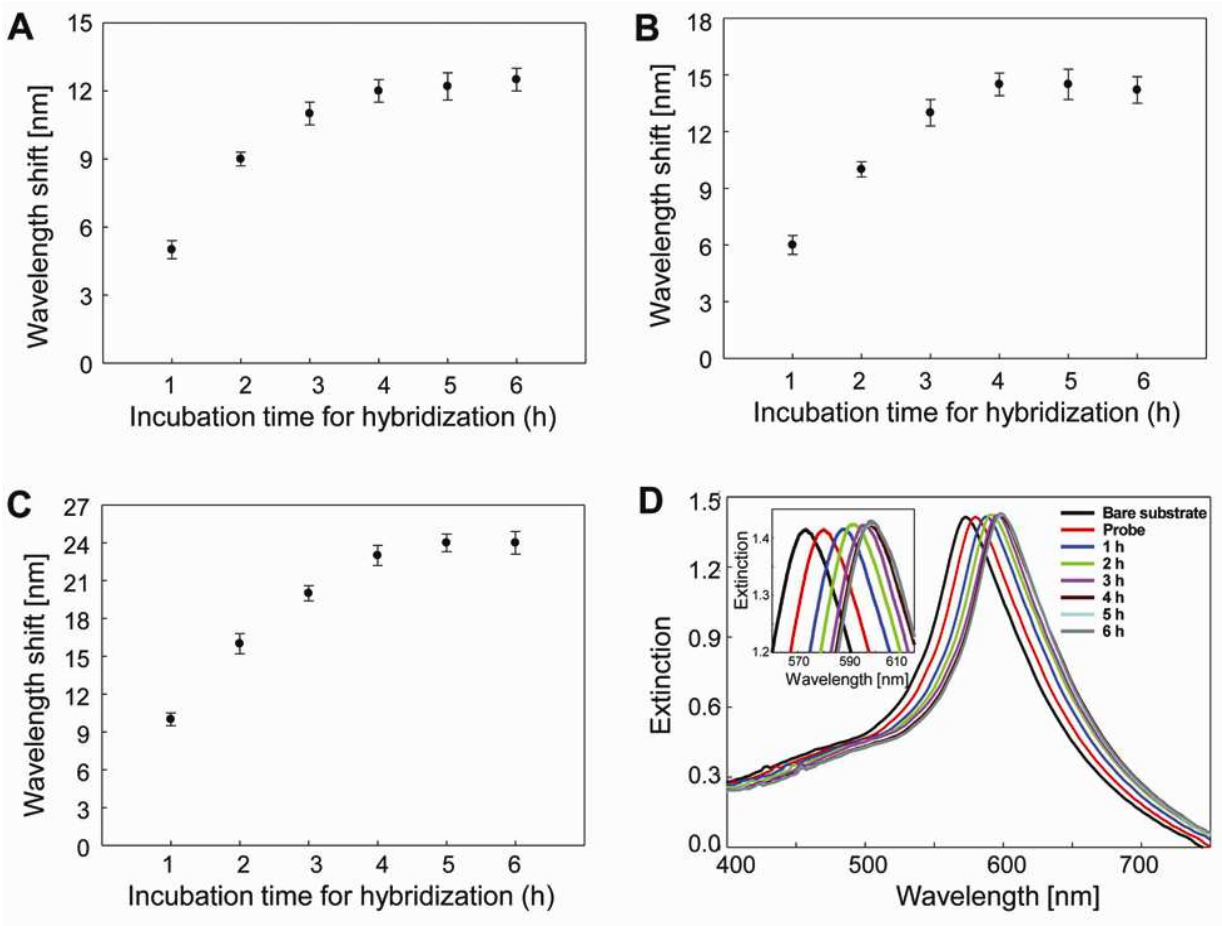

Figure S7. Effect of the incubation time of target DNAs on the LSPR wavelength shift. The chips were immobilized with the 10 μM probe DNAs for 4 h and hybridized with their complementary 1 μM target DNAs for various times (1, 2, 3, 4, 5 and 6 h). (A) *S. aureus*, (B) *K. oxytoca,* (C) *N. gonorrhoea.* (D) LSPR spectrum profiles of *N. gonorrhoea*-identifying sensor and the magnified spectrum profiles (inset). The data were obtained from three measurements and the error bars represent standard deviations.

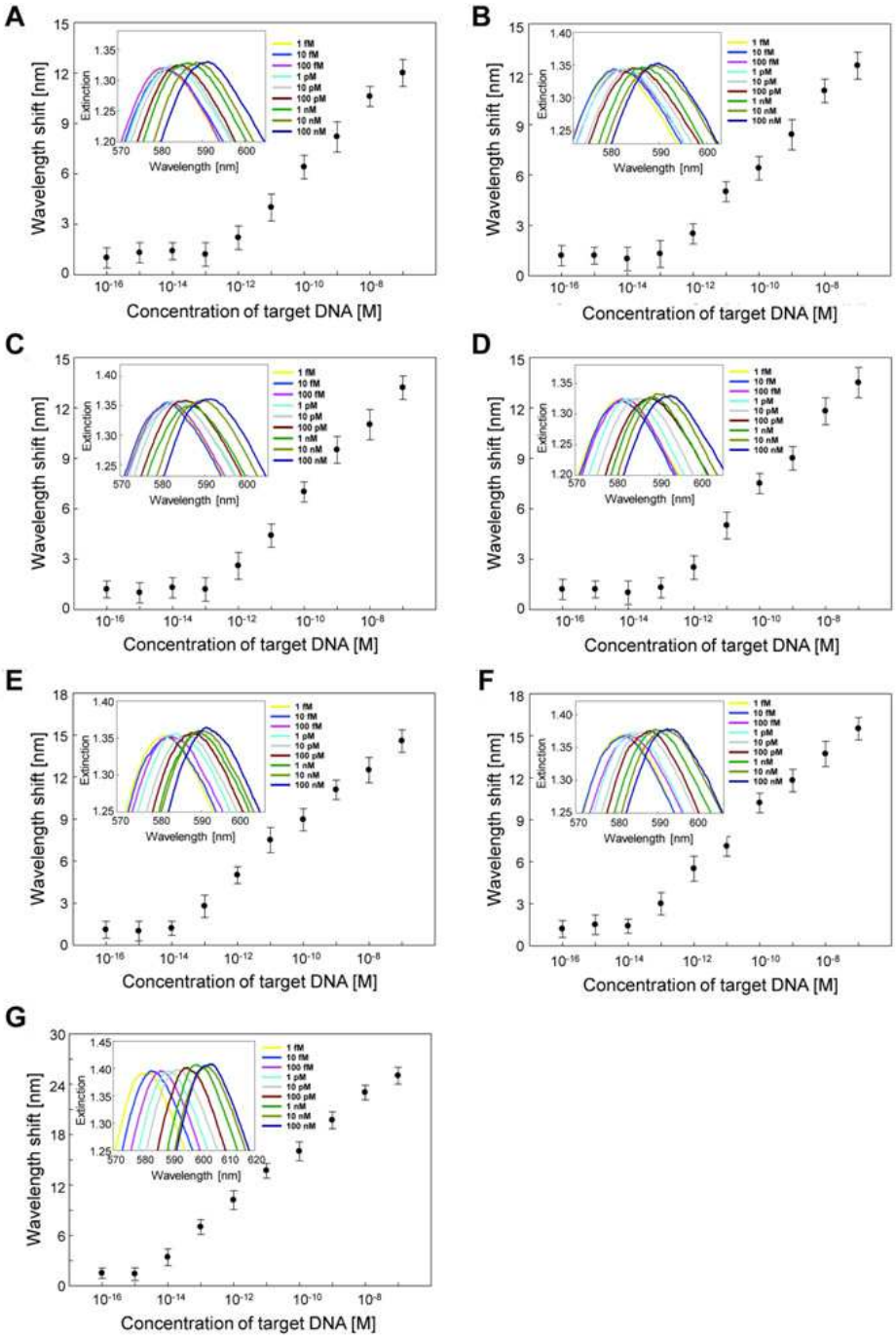

Figure S8. The detection limit of MC-NPA chip for DNA detection. Target DNAs were prepared by amplifying with species-specific primers and universal primers. The chips were applied with the different concentration (10^{-16} to 10^{-9} M) of target DNAs from seven reference bacteria as follows: (A) *V. vulnificus* (119-mer), (B) *Salmonella* spp. (138-mer), (C) *S. aureus* (194-mer), (D) *S. epidermidis* (202-mer), (E) *E. faecalis* (353-mer), (F) *K. oxytoca* (434-mer), and (G) *N. gonorrhoea* (1236-mer). The detection limit was determined by observing the red-shift of wavelength of chips. The graph of LSPR wavelength shift versus target DNA concentration shows linearly fitted line. The data was obtained from three measurements, and the error bars represent standard deviations. The insets represent LSPR spectrum profiles of each chip.

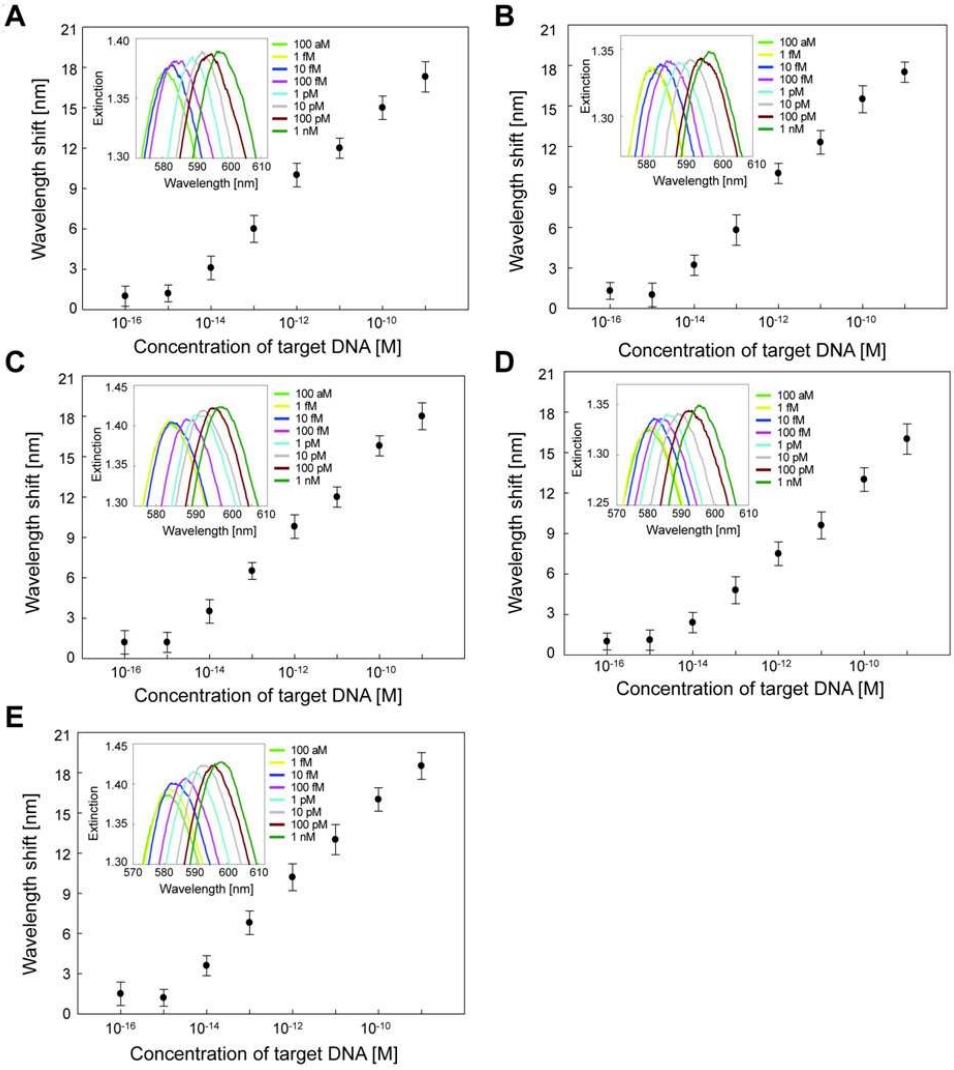

Figure S9. The detection limit of MC-NPA chips for DNA detection. Target DNAs were prepared by amplifying with universal primers. The chips were applied with the different concentration (10^{-16} to 10^{-9} M) of target DNAs from five reference bacteria as follows: (A) *V. vulnificus* (772-mer), (B) *Salmonella* spp. (791-mer), (C) *S. epidermidis* (757-mer), (D) *E. faecalis* (712-mer), and (E) *K. oxytoca* (900-mer). The detection limit was determined by observing the red-shift of wavelength of chips. The graph of LSPR wavelength shift versus target DNA concentration shows linearly fitted line. The data was obtained from three measurements, and the error bars represent standard deviations. The insets represent LSPR spectrum profiles of each chip.